

# A RESONANT DC LINK INVERTER FOR AN ELECTRIC VEHICLE

Zhenyue Hong, Richard Duke, Simon Round

Department of Electrical and Electronic Engineering  
University of Canterbury, New Zealand

Email: r.duke@elec.canterbury.ac.nz, s.round@elec.canterbury.ac.nz

## Abstract

This paper presents the development of a resonant DC link inverter for an electric vehicle application. The resonant link frequency is approximately 70kHz and the inverter drives a low voltage 2.2kW AC induction motor. The IGBT inverter operates off a 240V DC supply and an active clamping circuit limits the resonant bus voltage to 500V. A synchronized PWM scheme is used to modulate the resonant inverter. Experimental results showing the operation of the resonant inverter in motoring and regenerating modes are given. A performance comparison of hard switching and resonant inverters with respect to power losses and motor current THD is provided, and it is shown that at PWM frequencies greater than 10kHz the resonant inverter is more efficient.

## 1. INTRODUCTION

Usually electric vehicles utilize hard switching inverters (HSI) to drive their motors. The attractiveness of the hard switching inverter stems from its circuit simplicity and rugged control schemes. However, this type of inverter suffers from high switching losses, high switching stresses, and EMI (electromagnetic interference) problems.

To solve these problems, soft switching resonant DC link inverters have been proposed [1] [2]. In a resonant DC link inverter, the DC bus is controlled to oscillate at a high frequency so that the bus voltage goes through periodic zero crossings, thus setting up zero voltage switching conditions for all devices across the bus. The resonant DC link inverter has been shown to be a viable topology to realize high performance and high power density AC drives [3]. The application of the resonant DC link inverter has been actively considered by many manufacturers. Such resonant DC link inverters are now commercially available with power ratings up to 200kVA from a 3-phase 480V input source [4].

This paper presents the design, implementation, and experimental tests of a resonant DC link inverter for an electric vehicle application. For an electric vehicle application the inverter system must be able to handle bi-directional power flow. All the previously reported resonant link inverters [1-4] have only considered unidirectional operation in which there is no regenerative action. The resonant link inverter presented in this paper is designed to allow bi-directional current flow. The resonant link frequency is designed to be approximately 70kHz and the inverter drives a 90V<sub>L-L</sub> 2.2kW induction motor. The IGBT inverter operates off a 240V DC supply and an

active clamping circuit limits the bus voltage to less than 500V. Experimental results showing the operation of the resonant inverter in motoring and regenerating modes are given. A performance comparison of hard switching and resonant inverters with respect to power losses and motor current THD is provided, and it is shown that at PWM frequencies greater than 10kHz the resonant inverter is more efficient.

## 2. OPERATING PRINCIPLES

Figure 1 shows the circuit schematic of an actively clamped resonant DC link inverter (ACRLI) [2]. A resonant network,  $L_r$ - $C_r$ , is added to the DC bus of a hard switching PWM inverter. The resonant link is excited by turning on all the devices in the inverter stage ( $S_1$ - $S_6$ ) so that the resonant inductor current,  $i_{Lr}$ , builds up. The resonant inductor current must be built up to a value that equals the required load current,  $i_x$ , plus a small current,  $I_T(\text{min})$ , that is required to overcome the resonant link losses. If the inductor current does not reach this level then the resonant link may not resonant back to zero volts and resonance

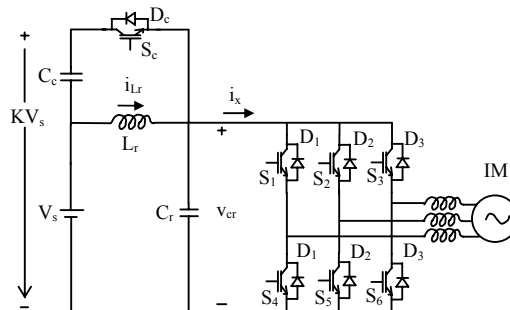


Figure 1. An actively clamped resonant DC link inverter.

failure will occur. Under normal operation once the bus voltage,  $v_{cr}$ , returns to zero volts, all the devices can be turned on again so as to maintain the resonant operation.

In the absence of an active clamping circuit ( $S_c$ ,  $D_c$  and  $C_c$ ), the peak bus voltage may shoot up when the inverter DC current,  $i_x$ , decreases abruptly due to the switching of the inverter devices. With the clamping circuit, the peak bus voltage can be limited to a clamping voltage,  $KV_s$ . To achieve this the capacitor  $C_c$  is precharged to a voltage of  $(K-1)V_s$  by an external flyback converter. The value of  $C_c$  is chosen so that the capacitor voltage only changes by a few volts when the resonant current flows in it. When the bus voltage reaches  $KV_s$ , the diode  $D_c$  is forward biased and clamps the bus voltage to  $KV_s$ . When  $D_c$  conducts, the device  $S_c$  is also turned on. The charge transferred to the clamp capacitor,  $C_c$ , when  $D_c$  conducts is recovered when  $S_c$  conducts. When the net charge transferred to  $C_c$  equals zero,  $S_c$  is turned off, and the  $L_r$ - $C_r$  circuit continues to resonate until the bus voltage reaches zero volts.

### 3. SIMULATIONS

Simulations were performed for the ACRLI with a three-phase load. The load is simply assumed to be a three-phase sinusoidal current source with a current rating of 25Arms at 50Hz, which is nominal motor current. All the components are assumed to be ideal. The DC supply is 240V, and the clamping voltage is set to 440V. The resonant inductor is  $20.45\mu\text{H}$ , the resonant capacitor is  $0.234\mu\text{F}$ , and the clamp capacitor is  $2200\mu\text{F}$ . These are all typical values for use in a resonant link.

Figure 2 shows the simulated waveforms of the ACRLI operating in the motoring mode. When the inverter DC current increases at a time of  $158\mu\text{s}$ , the time required for the charging of the resonant inductor becomes longer. However, when the inverter DC current decreases at a time of  $116\mu\text{s}$ , no inductor charging time is required as indicated by the bus voltage being zero for a very short time. In this case of a current decrease the voltage clamping time must become longer to absorb the additional energy. With the use of the clamping circuit the peak bus voltage is limited to the clamping voltage of 440V, reducing the voltage stresses on the inverter devices. The "saw-tooth" shapes appearing periodically in the waveform of the inverter DC current indicate that all the antiparallel diodes in the inverter stage ( $D_1$ - $D_6$ ) conduct first and clamp the bus voltage to zero when the bus voltage reaches zero volts, then the switching devices are turned on for the inductor charging. Note that although the inverter devices are involved with maintaining the link resonance, the additional current

stresses on these devices are seen to be minimal. Also, it is noted that the changes in the inverter DC current occur only during zero voltage intervals, demonstrating the zero voltage switching of the inverter devices. The top trace in Figure 2 is the predicted inverter DC current, which is the reference signal for the inductor charging control.

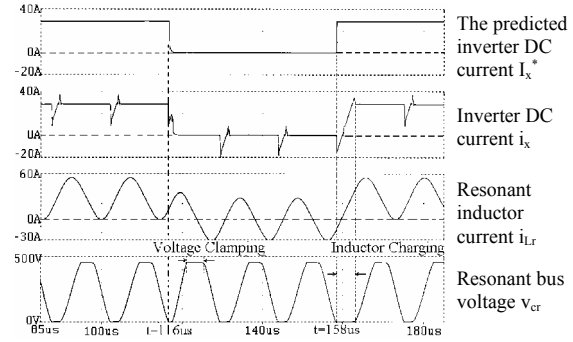


Figure 2. Simulated waveforms of the ACRLI operating in the motoring mode.

Figure 3 shows the simulated waveforms of the ACRLI operating in the regenerating mode. It can be seen that the resonant link remains resonating even when the inverter DC current is reversed.

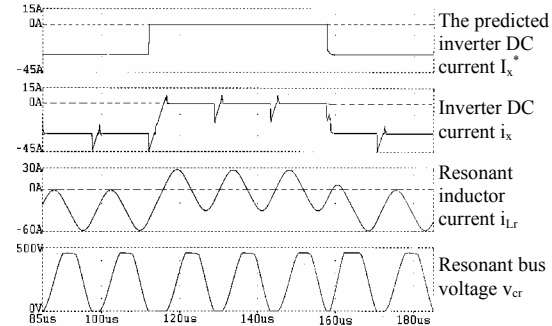


Figure 3. Simulated waveforms of the ACRLI operating in the regenerating mode.

### 4. DESIGN

In the resonant DC link inverter, the low loss switching of the inverter devices is accomplished at the expense of the link losses. Given the device characteristics, the link components can then be designed to minimize the total inverter losses.

Figure 4 shows the design optimization curves for the resonant DC link inverter using IGBTs (BSM50GD60DN2, Siemens) operated off a DC supply of 240V. For loss calculations the inverter load is assumed to be a sinusoidal current source of 25A rms with a power factor 0.86. The link frequency of 70kHz is used, as this value is adequate to preserve the resolution of sinusoidal PWM signals according to simulations. Losses in the resonant capacitor and clamp capacitor are neglected because they are very low.

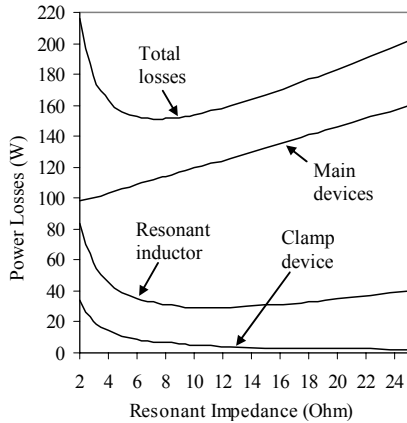


Figure 4. Variation of the losses in the ACRLI due to the resonant impedance.

A small resonant impedance indicates that a large value of the resonant capacitance is required and this results in a slow increase of the bus voltage when the main devices are switched off. This means there is a small voltage across the main switching devices as they are turned off and this results in low switching losses in the main devices. However, a small value of the resonant impedance causes a large circulating current in the resonant link and high losses in the resonant inductor and the clamp device. From Figure 4 it can be seen that for the given application the optimum value of the resonant impedance is around  $8.5\Omega$ . With the link frequency of  $70\text{kHz}$ , this optimum value corresponds to a resonant inductance of  $19.2\mu\text{H}$  and a resonant capacitance of  $0.267\mu\text{F}$ . In practice the required resonant capacitance is obtained by paralleling several small film capacitors, therefore only the discrete values of the resonant capacitance can be obtained. For this reason, the closest values of the resonant inductance of  $20.45\mu\text{H}$  and the resonant capacitance of  $0.234\mu\text{F}$  are used to implement the prototype resonant DC link inverter.

Table 1 summarizes the component values used for the prototype resonant inverter. One IGBT module is used to form one phase leg of the resonant inverter. In order to handle the peak load current of  $106\text{A}$ , the top and bottom three IGBTs in each module are paralleled to obtain a current rating of  $150\text{A}$ . Similarly, the top three IGBTs in one module are paralleled and used as the clamp device.

Table 1. Components for the prototype ACRLI

$S_1$ - $S_6$ / $D_1$ - $D_6$	50A/600V IGBT module per phase leg
$S_c$ / $D_c$	50A/600V IGBT module
$L_r$	$20.45\mu\text{H}$ , core PM114/93 N27, 5 turns Litz wire, air gap 2.6mm
$C_r$	$0.234\mu\text{F}$ , $5 \times 0.047\mu\text{F}$ 1000VDC, polypropylene capacitors in parallel
$C_c$	$2200\mu\text{F}$ , $2 \times 1100\mu\text{F}$ 350VDC electrolytic capacitors in parallel

## 5. CONSTRUCTION

Simulations of the ACRLI modelled with the stray inductance reveal that the interaction between the resonant capacitor and the stray inductance may lead to the non-zero voltage switching of the inverter devices during the bus shorting and to bus voltage overshoot during the active clamping. Minimization of the stray inductance is important when designing the physical layout of the ACRLI (Figure 5). A laminated bus structure is incorporated into the inverter assembly, and the resonant capacitors are embedded directly into the laminated bus structure so that the stray inductance associated with the circuit loop from the resonant capacitor to the inverter stage and return is minimized. Supply capacitors ( $2 \times 1100\mu\text{F}$ ) are included in the inverter assembly to offset the stray inductance of the long cables from the inverter to the DC supply. The clamp capacitors are placed as close as possible to the supply capacitors and the clamp device so as to minimize the stray inductance associated with the interconnections and reduce the bus voltage overshoot during the active clamping. The constructed resonant inverter can be easily configured as a hard switching inverter; this allows an experimental comparison of the power losses in the resonant and hard switching inverters for the same inverter devices.

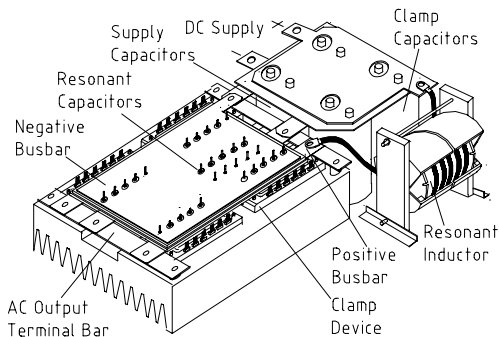


Figure 5. Physical layout of the prototype ACRLI.

## 6. CONTROL

When the resonant DC link inverter operates with a load, the resonant link can be subjected to severe inverter DC current transitions. In order to maintain link resonance, it is necessary to ensure that a proper initial current is established in the resonant inductor at the beginning of every resonant cycle.

A block diagram of the inductor charging control is shown in Figure 6, and the related waveforms are shown in Figure 7. Whenever the resonant bus voltage is less than a reference voltage,  $V_{\text{check}}$ , a sampling pulse,  $P_{\text{sample}}$ , is generated. Sinusoidal PWM

signals (A+, A-, B+, B-, C+ and C-), generated by comparing a triangular signal with a three-phase sinusoidal zero reference, are sampled and held prior to the zero crossing by means of a flip-flop (FF1). The sampled signals (a+, b+ and c+) are then fed to a predictor, which is also supplied with motor phase currents,  $i_a$  and  $i_c$  [5]. Knowing the new switching signals of the inverter and the information regarding the motor currents, the predictor yields a predicted inverter DC current for the next resonant cycle,  $I_x^*$ , before the zero crossing as shown in Figure 7.

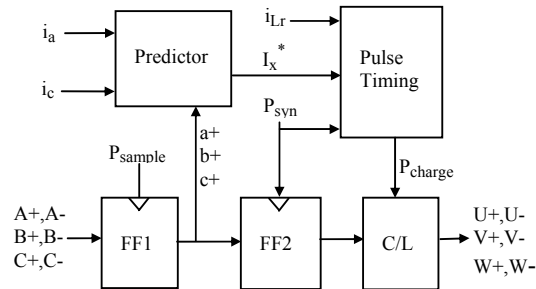


Figure 6. Block diagram of inductor charging control.

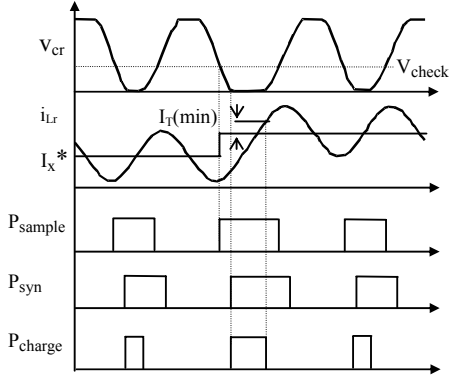


Figure 7. Waveforms for the current prediction.

Once the bus voltage reaches zero volts, a pulse,  $P_{syn}$ , is produced and used to transfer the sampled PWM signals to a combination logic circuit by means of a second flip-flop (FF2). Meanwhile,  $P_{syn}$  triggers a timing circuit that generates an inductor charging pulse,  $P_{charge}$ . Through the combination logic circuit and IGBT gate drives, the inductor charging pulse is applied to all the inverter devices to accomplish the bus shorting. With the bus shorted, the inductor current,  $i_{Lr}$ , is linearly increased, and the control circuit continuously compares the inductor current with the predicted inverter DC current. Once the inductor current is larger than the predicted inverter DC current by the value of the minimum loss current,  $I_T(min)$ , the control circuit terminates the inductor charging pulse immediately and releases the bus shorting. Upon releasing the bus shorting, the gate drives are updated with the new switching signals, and the resonant inverter begins the next resonant cycle.

## 7. EXPERIMENTAL RESULTS

The experimental setup for the tests of the resonant inverter loaded with an induction motor is shown in Figure 8. The DC supply is obtained from AC mains through a variac and a rectifier. The motor can be loaded by prony brake. The motor has a rated power of 2.2kW, a rated line-to-line voltage of 90V rms, and a rated frequency of 50Hz.

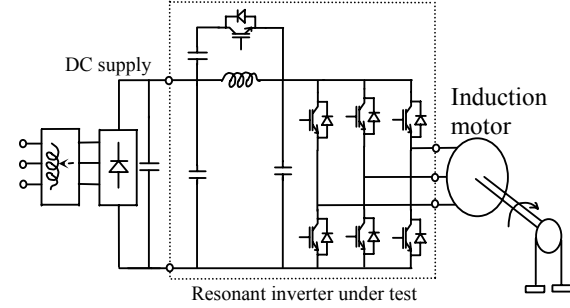


Figure 8. Experimental setup.

### A. INVERTER OPERATION

Figures 9 and 10 show the measured waveforms of the resonant inverter operated with the induction motor under full load conditions. For the tests, the DC supply voltage was 240V, the clamping voltage was set to 440V, and the inverter delivered a phase current of 20.5A rms at 50Hz into the induction motor.

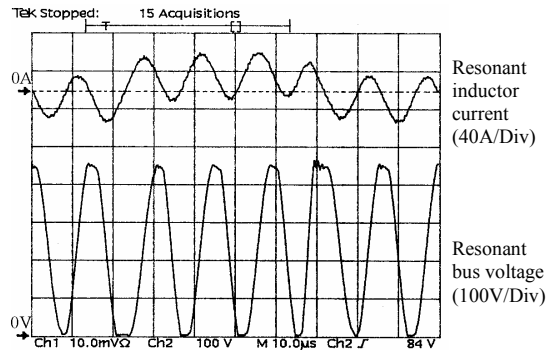


Figure 9. Link waveforms under full motor load

From Figure 9 it can be seen that although the inductor current varies with the changes in the inverter DC current, the resonant pulses of the bus voltage are stable from cycle to cycle. With the active clamping circuit the peak bus voltage is well restricted below 500V allowing a sufficient voltage margin for the 600V IGBTs. The maximum peak bus voltage is about 468V, an overshoot of 28V above the clamping voltage due to the stray inductance. The bus-shortening interval also varies with the inverter DC current, and the average link frequency is approximately 70kHz. Under these operating conditions, the rms current in the resonant inductor is 21.6A, and the peak current is

54A. Shown in Figure 10, the upper trace is the output phase current, and the lower trace is the output line-to-line voltage, which is synthesised with the low dv/dt resonant pulses of the bus voltage.

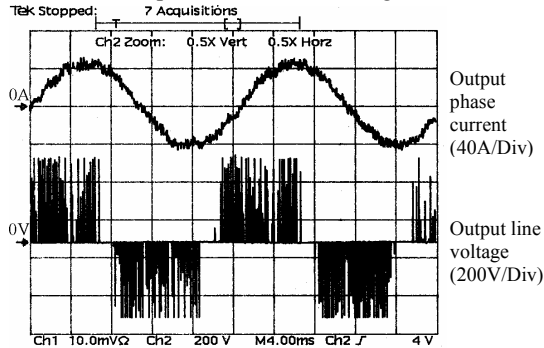


Figure 10. Output waveforms under full load

An electric vehicle requires frequent regeneration, where energy is fed back to the battery bank by the motor to maximize the usage of battery energy. The regeneration tests of the ACRLI were carried out by slowing down the motor from 70Hz to 30Hz with a deceleration rate of 10Hz/s. Figure 11 shows the measured link waveforms in the regenerating mode. It is clear that the regenerated energy from the motor is fed back to the DC supply. It can be seen that the average value of the resonant inductor current is negative and the bus voltage has stable resonant pulses implying that no energy is accumulated in the resonant capacitor during the regeneration.

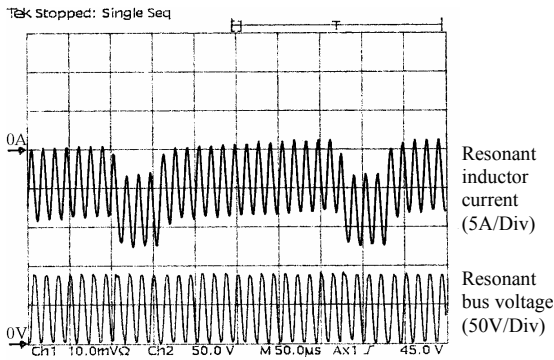


Figure 11. Link waveforms in the regenerating mode.

## B. POWER LOSSES

A thermal method was used to measure the total power losses of the resonant DC link inverter and the same inverter operating with hard switching. The whole inverter system including the gate drives was enclosed in a thermal box. By measuring the temperature rise inside the thermal box, loss measurements are obtained from a calibration curve of the thermal box. Figure 12 plots the measured power losses of the resonant DC link inverter and the hard switching inverter as a function of PWM switching frequency. For these measurements, the inverters

were both operated with the induction motor under full load conditions.

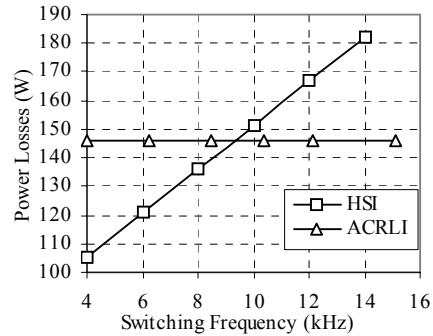


Figure 12. Total losses of the HSI and ACRLI as a function of PWM switching frequency.

For the hard switching inverter, the total losses increase linearly with the PWM switching frequency for a constant load current. The total losses in the HSI are in the range of 105W to 182W for a PWM frequency range from 4kHz to 14kHz. In the HSI the measured total losses consist of the conduction losses, switching losses, and the gate drive losses. Assuming that the conduction losses and gate drive losses are constant, and the switching losses have a linear relationship with the PWM switching frequency, then the conduction and switching losses can be obtained separately from the measured data. Switching losses of 106W are found in the HSI at 14kHz.

In contrast, the total losses in the resonant inverter are constant at 146W with the increase of the PWM switching frequency. This result strongly demonstrates that the zero voltage switching in the resonant DC link inverter decouples the device losses from the PWM switching frequency. The resonant inverter shows a noticeable loss reduction over the HSI at the PWM switching frequencies greater than 10kHz. Comparing the measured losses at 14kHz for the HSI and 15kHz for the ACRLI, the ACRLI has a power saving of 36W attributed to the significantly reduced switching losses. That is about 20% of the total losses in the HSI at 14kHz. Accounting for the resonant link losses of 47W measured from the resonant inverter under no load, it can be said that the switching losses of 83W out of 106W in the HSI at 14kHz have been eliminated. That is an elimination of the 78% switching losses in the main devices by the zero voltage switching compared to the hard switching.

## C. MOTOR CURRENT DISTORTION

The total harmonic distortion (THD) of the motor current was measured for the HSI and the ACRLI for PWM switching frequencies from 4kHz to 15kHz. For all measurements, the inverters were both

operated with the induction motor under full load conditions. The measured THD value includes the first 20 harmonics of the fundamental frequency of 50Hz. Figure 13 shows the measured results. It can be seen that at some distinct PWM switching frequencies, the resonant inverter modulated by the synchronized PWM scheme causes much higher THD values in the motor current compared to the HSI modulated by the conventional PWM scheme. These PWM switching frequencies happen to be the  $1/N$  of the link frequency of 70kHz ( $N$  is an integer). This phenomenon is due to the sampling of the sinusoidal PWM signals. For example, a sinusoidal PWM signal at approximately 14kHz contains harmonic components with the 5<sup>th</sup> harmonic being close to 70kHz. The modulation of this with the resonant frequency of 70kHz causes low frequency distortion in the motor current. However, except at the PWM switching frequencies in the vicinity of those distinct frequency points, the THD values of the motor current for the ACRLI are in the range of 3-4%, and they are very comparable to those for the HSI, which are in the range of 2-3%.

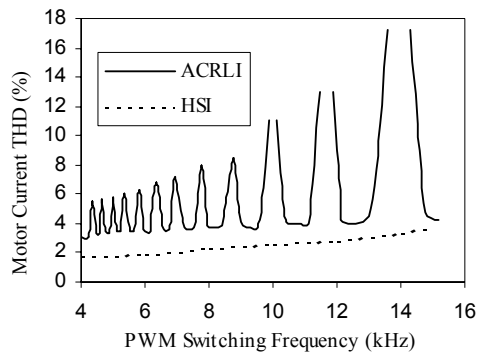


Figure 13. THD of the motor current in the HSI and ACRLI versus PWM switching frequency.

## 8. CONCLUSIONS

A resonant DC link inverter driving a 2.2kW induction motor for an electric vehicle application has been developed. Inverter operation with a 240V DC supply at a link frequency of approximately 70kHz has been successfully demonstrated. It has been experimentally confirmed that the resonant DC link inverter is capable of bi-directional power flow. Inverter tests have shown that the resonant DC link inverter has the advantages of low losses, a low  $dv/dt$ , low acoustic noise, a high switching frequency, and snubberless operation. Therefore, the resonant DC link inverter has a promising application to electric vehicle propulsion.

## 9. REFERENCES

- [1]. Divan D.M., "The Resonant DC Link Converter-A New Concept in Static Power Conversion," *IEEE Trans. Ind. App.*, vol. 25, pp. 317-324, Mar/April, 1989.
- [2]. Divan D.M., Skibinski G., "Zero-Switching-Loss Inverters for High-Power Applications," *IEEE Trans. Ind. App.*, vol. 25, pp. 634-643, July/Aug, 1989.
- [3]. Mertens A., Divan D.M., "A High Frequency Resonant DC Link Inverter Using IGBTs," in *IPEC'90 Rec.*, pp. 152-160, 1990.
- [4]. Divan D.M., Wallace I., "New Developments in Resonant DC Link Inverters," *Conf. Rec. PCC'97-Nagaoka*, pp.311-318, 1997.
- [5]. Deshpande V.V., Doradla S.R., Divan D.M., "A Current-Prediction Scheme for the PRDCL Inverter-Fed Induction Motor Drive," *IEEE Trans. Power Electron.*, vol. 12, pp. 64-70, Jan, 1997.